



# Preclinical PET Neuroimaging of [<sup>11</sup>C]Bexarotene

Benjamin H. Rotstein, PhD<sup>1,2</sup>, Michael S. Placzek, PhD<sup>2,3,4</sup>,  
Hema S. Krishnan, PhD<sup>1,2</sup>, Aleksandra Pekošak, MPharm<sup>1,2</sup>,  
Thomas Lee Collier, PhD<sup>1,2,5</sup>, Changning Wang, PhD<sup>2,3</sup>, Steven H. Liang, PhD<sup>1,2</sup>,  
Ethan S. Burstein, PhD<sup>6</sup>, Jacob M. Hooker, PhD<sup>2,3</sup>, and Neil Vasdev, PhD<sup>1,2</sup>

## Abstract

Activation of retinoid X receptors (RXRs) has been proposed as a therapeutic mechanism for the treatment of neurodegeneration, including Alzheimer's and Parkinson's diseases. We previously reported radiolabeling of a Food and Drug Administration-approved RXR agonist, bexarotene, by copper-mediated [<sup>11</sup>C]CO<sub>2</sub> fixation and preliminary positron emission tomography (PET) neuroimaging that demonstrated brain permeability in nonhuman primate with regional binding distribution consistent with RXRs. In this study, the brain uptake and saturability of [<sup>11</sup>C]bexarotene were studied in rats and nonhuman primates by PET imaging under baseline and greater target occupancy conditions. [<sup>11</sup>C]Bexarotene displays a high proportion of nonsaturable uptake in the brain and is unsuitable for RXR occupancy measurements in the central nervous system.

## Keywords

bexarotene, carbon-11, positron emission tomography, retinoid X receptor, neuroimaging

## Introduction

Bexarotene is a potent retinoid X receptor (RXR) agonist that has shown potential for treating Parkinson's disease (PD), possibly through its ability to activate RXR-Nurr1 heterodimers,<sup>1</sup> and been demonstrated to induce β-amyloid clearance from a murine model of Alzheimer's disease (AD).<sup>2</sup> However, as bexarotene was developed to treat dermatological diseases and certain cancers such as cutaneous T-cell lymphoma (CTCL),<sup>3</sup> there is scant pharmacokinetic and pharmacodynamic data describing bexarotene in the central nervous system (CNS). Recently, bexarotene was shown to reduce brain amyloid in ApoE4 noncarriers diagnosed with AD, providing further evidence that bexarotene is indeed CNS active.<sup>4</sup> However, in that study, only a relatively high dose of bexarotene was tested, and significant elevations in triglycerides were observed in all patients treated. Furthermore, the Food and Drug Administration-approved bexarotene dosage to treat CTCL causes side effects and may present tolerability problems in patients with PD and AD.<sup>5,6</sup>

Bexarotene may have neuroprotective effects at doses that are substantially lower than effective doses for treating cancer,<sup>1</sup> and it has been shown that "low-dose" bexarotene is well tolerated clinically and likely has CNS activity.<sup>7,8</sup> Low-dose treatment rescued dopamine (DA) neurons and restored behavioral function in 6-hydroxydopamine (OHDA)-lesioned rats.<sup>1</sup> The brain-

to-plasma ratio of bexarotene in rats was approximately 1:1. The minimum effective steady-state brain concentration for the protection of DA neurons in 6-OHDA-lesioned rats was approximately 40 nmol/L, whereas the peak brain concentration of bexarotene at the minimum effective oral dose of 1 mg/kg/d was approximately 400 nmol/L. Thus, it remains unclear what dose of bexarotene would provide the optimal ratio of CNS activity-related side effects arising from peripheral exposure.

To resolve uncertainties about dose selection of bexarotene and other Nurr1-RXR agonists for patients with PD, we sought

<sup>1</sup> Division of Nuclear Medicine and Molecular Imaging, Gordon Center for Molecular Imaging, Massachusetts General Hospital, Boston, MA, USA

<sup>2</sup> Department of Radiology, Harvard Medical School, Boston, MA, USA

<sup>3</sup> Athinoula A. Martinos Center for Biomedical Imaging, Massachusetts General Hospital, Charlestown, MA, USA

<sup>4</sup> Department of Psychiatry, McLean Imaging Center, McLean Hospital, Belmont, MA, USA

<sup>5</sup> Advion, Inc, Ithaca, NY, USA

<sup>6</sup> ACADIA Pharmaceuticals, Inc, San Diego, CA, USA

Submitted: 31/03/2016. Revised: 01/06/2016. Accepted: 06/07/2016.

## Corresponding Authors:

Neil Vasdev and Benjamin H. Rotstein, Massachusetts General Hospital, Harvard Medical School, 55 Fruit Street, Boston, MA 02114, USA.

E-mails: vasdev.neil@mgh.harvard.edu; benjamin.rotstein@uottawa.ca



to evaluate the potential for measuring occupancy of midbrain RXRs by positron emission tomography (PET) with [ $^{11}\text{C}$ ]bexarotene. Our preliminary work established both the feasibility of chemical synthesis of [ $^{11}\text{C}$ ]bexarotene and its utility for imaging the midbrain in a nonhuman primate (NHP) in vivo using PET.<sup>9</sup> In addition to [ $^{11}\text{C}$ ]bexarotene, retinoid A receptor ligands have been radiolabeled with carbon-11,<sup>10,11</sup> and more recently, a fluorine-18-labeled bexarotene analog has been reported.<sup>12</sup> However, to date, there are no reports exploring the specificity of these ligands for molecular imaging. Bexarotene displays comparable affinities toward RXR $\alpha$ ,  $\beta$ , and  $\gamma$  (14, 21, and 29 nmol/L, respectively)<sup>3</sup> and may have greater affinity toward RXR heterodimers, such as Nurr1-RXR.<sup>1</sup> Retinoid X receptor subtypes are expressed differentially in mammalian organs<sup>13</sup> and brain regions,<sup>14</sup> with each exhibiting specific patterns of localization. Estimates of  $B_{\text{max}}$  in the brain have not been made, although values ranging from 0.346 to 0.567 pmol/mg in rat liver nuclear proteins have recently been reported.<sup>15</sup> An in vivo probe for CNS RXRs would serve as a powerful tool in drug development in the context of neurodegenerative diseases. In this brief report, we evaluate the potential of [ $^{11}\text{C}$ ]bexarotene for neuroimaging of RXRs in rats and NHPs by in vivo PET imaging.

## Materials and Methods

All treatment and imaging experiments were conducted according to procedures approved by the Institutional Animal Care and Use Committee at Massachusetts General Hospital. [ $^{11}\text{C}$ ]Bexarotene was synthesized from [ $^{11}\text{C}$ ]CO<sub>2</sub>, as previously described<sup>9</sup> with minor modifications. A total of 9 radiosyntheses were completed for this study with radiochemical purity  $\geq 98\%$  and specific activities of  $55 \pm 5$  mCi/ $\mu\text{mol}$  measured at end-of-synthesis. The range of isolated yields was 5.6 to 36.9 mCi.

### Plasma Protein Binding

An aliquot of [ $^{11}\text{C}$ ]bexarotene formulated in 8% ethanolic saline with 4% Tween 80 ( $\sim 100$   $\mu\text{L}$ , 100  $\mu\text{Ci}$ ) was added to a sample of baboon plasma (500  $\mu\text{L}$ , freshly prepared by centrifugation of freshly drawn blood), diluted with water (100  $\mu\text{L}$ ). The mixture was gently combined by repeated inversion and incubated for 10 minutes at room temperature. Aliquots (3, 20  $\mu\text{L}$  each) were withdrawn into test tubes to determine the total radioactivity in the plasma ( $A_{\text{T}}$ ). An additional 300  $\mu\text{L}$  of the incubated plasma sample was withdrawn and placed into the upper compartment of a Centrifree ultrafiltration device (Amicon, Inc, Beverly, Massachusetts). The device was centrifuged for 10 minutes, after which the upper compartment was removed and discarded. Aliquots (3, 20  $\mu\text{L}$  each) from the collection cup were withdrawn into test tubes to determine the fraction of radioactivity that passed through the membrane ( $A_{\text{unbound}}$ ). All  $A_{\text{T}}$  and  $A_{\text{unbound}}$  test tubes were counted sequentially in a well counter with decay correction. Empty test tubes served as background samples. The above procedure was performed in duplicate. Plasma protein binding

is reported as the bound fraction of radioactivity ( $A_{\text{bound}}/A_{\text{T}} = 1 - A_{\text{unbound}}/A_{\text{T}}$ ).

## Positron Emission Tomography Imaging

### Rodents

Male Sprague Dawley rats ( $n = 4$ , 440-500 g) were anesthetized by inhalation of 3% isoflurane in a carrier of 1.5 L/min medical oxygen and maintained at 2% isoflurane for the duration of the scan. The rats were arranged in quadrants of a Siemens P4 small animal PET scanner (Siemens Preclinical Solutions, Knoxville, TN). Nonradioactive bexarotene (1 mg/kg,  $n = 2$ ) or vehicle (10% dimethyl sulfoxide, 4% Tween 80, saline, 440-500  $\mu\text{L}$ ,  $n = 2$ ) was injected via a lateral tail vein catheter 5 minutes prior to radiotracer administration ([ $^{11}\text{C}$ ]bexarotene, 220-240  $\mu\text{Ci}$ , 310-350  $\mu\text{L}$ ) by the same route. Dynamic PET acquisition lasted for 60 minutes from the time of radiotracer injection, followed by a transmission scan with a  $^{57}\text{Co}$  line source to generate an attenuation map, which was applied during image reconstruction. The dynamic PET data were binned into 32 time frames (8  $\times$  15 seconds, 8  $\times$  60 seconds, 10  $\times$  120 seconds, and 6  $\times$  300 seconds) and reconstruction of each frame via an iterative maximum likelihood expectation maximization algorithm, consisting of 16 iterations, afforded images with a resolution of approximately 2-mm full width at half-maximum. Images were analyzed using AMIDE 1.0.4 software (<http://amide.sourceforge.net>). Whole-brain volumes of interest (VOIs) were drawn over each image to derive time-activity curves.

### Nonhuman Primates

Positron emission tomography/magnetic resonance imaging (MRI) acquisition was performed on a 3-T Siemens TIM-Trio with a BrainPET insert (Siemens, Erlangen, Germany). A PET/MRI-compatible 8-channel array coil customized for NHP brain imaging to increase signal and quality was used. Two baboons (15.1-16.4 kg) were used for baseline and non-radioactive bexarotene coadministration (0.35-0.42 mg/kg, intravenously [IV]; high occupancy) imaging conditions. During administration of [ $^{11}\text{C}$ ]bexarotene (3.8-5.0 mCi), dynamic PET image acquisition was initiated and data were collected and stored in list mode for 90 minutes. Positron emission tomography data were binned into 26 time frames (6  $\times$  10 seconds, 6  $\times$  20 seconds, 2  $\times$  30 seconds, 1  $\times$  60 seconds, 5  $\times$  300 seconds, and 6  $\times$  600 seconds). Image reconstruction was performed using the 3-dimensional ordinary Poisson expectation maximization algorithm with detector efficiency, decay, dead time, attenuation, and scatter corrections. Image volumes were eventually reconstructed into 76 slices with 128  $\times$  128 pixels and a 2.5-mm isotropic voxel size. Thirty minutes after scanner start, a high-resolution anatomical scan using multiecho MPRAGE sequence (repetition time [TR] = 2530 milliseconds, echo time [TE]1/TE2/TE3/TE4 = 1.64/3.5/5.36/7.22 milliseconds, T1 = 1200 milliseconds, flip angle = 7°, and 1 mm isotropic) was acquired. Image analysis was conducted

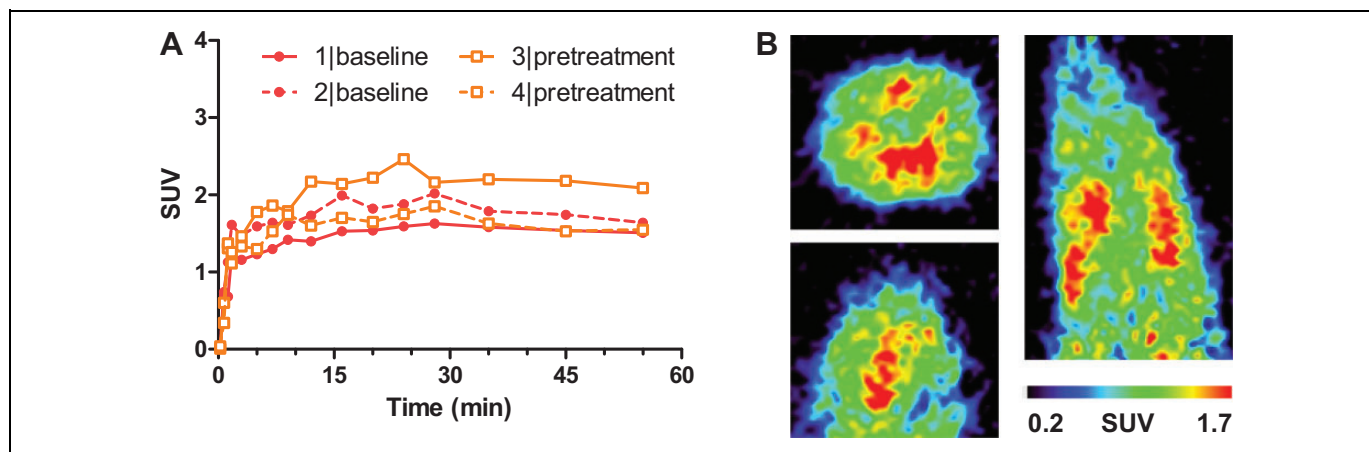


**Figure 1.** A, Whole-brain time-activity curves of [ $^{11}\text{C}$ ]bexarotene in rat at baseline ( $n = 2$ ) and following pretreatment (bexarotene 1.0 mg/kg, IV, 5 minutes prior to TOI,  $n = 2$ ). B, Summed PET images at baseline 2 to 60 minutes; clockwise from top left: transverse, sagittal, and coronal slices. IV indicates intravenously; PET, positron emission tomography; TOI, time of injection.

using the PMOD 3.3 (PMOD Technologies, Zurich, Switzerland) software package. Six VOIs were drawn including whole brain, cerebellum, frontal cortex, prefrontal cortex, thalamus, and caudate to derive time-activity curves.

## Results

[ $^{11}\text{C}$ ]Bexarotene was prepared by copper-mediated [ $^{11}\text{C}$ ]CO $_2$  fixation from a pinacol ester boronate precursor,<sup>16,17</sup> as described previously.<sup>9</sup> The average injected dose of [ $^{11}\text{C}$ ]bexarotene was  $232 \pm 8 \mu\text{Ci}$  ( $3.0 \pm 1.0 \mu\text{g}/\text{kg}$ ) for rats and  $4.27 \pm 0.51 \text{ mCi}$  ( $1.8 \pm 0.2 \mu\text{g}/\text{kg}$ ) for primates.

Whole-brain radioactivity uptake was determined in rats at baseline and with homologous pretreatment to evaluate binding saturability. Whole-brain activity peaked within the first 2 minutes after injection of [ $^{11}\text{C}$ ]bexarotene to rats at baseline and then reached  $\sim 2$  standardized uptake value (SUV) with little further clearance over the duration of the 60-minute scan (Figure 1). Pretreatment with nonradioactive bexarotene (1 mg/kg, IV, 5 minutes prior to the time of injection [TOI]) effected no measurable change in whole-brain radioactivity uptake.

To assess regional uptake specificity in various brain structures and in order to mitigate the possible confound of species differences, PET neuroimaging with [ $^{11}\text{C}$ ]bexarotene was further evaluated in NHPs. Our preliminary study demonstrated moderate brain uptake of [ $^{11}\text{C}$ ]bexarotene at baseline with regional heterogeneity.<sup>9</sup> In the current study, we confirmed [ $^{11}\text{C}$ ]bexarotene brain uptake and distribution at baseline ( $n = 2$ ) and also conducted imaging with coadministration of nonradioactive drug ( $n = 2$ ) to observe changes that would indicate saturable binding. As in our preliminary study, whole-brain uptake peaked at  $\sim 0.8$  SUV, 8 to 12 minutes after TOI (Figure 2). A similar pattern of distribution throughout the brain was observed, with relatively high uptake notably in the cerebellum, frontal cortex, prefrontal cortex, thalamus, and caudate. In vitro plasma protein binding was determined from a freshly drawn blood sample, and [ $^{11}\text{C}$ ]bexarotene was found

to be highly protein bound ( $>99\%$ ), in line with previous reports in other species.<sup>18</sup> Drug coadministration studies showed no measurable change in whole-brain or regional uptake of [ $^{11}\text{C}$ ]bexarotene over the duration of the 90-minute scans. No differences in regional heterogeneity were observed between baseline and coadministration scan images.

## Discussion

Neuroreceptor imaging by PET requires radiotracers that engage in specific and saturable binding to the target of interest. In vivo target saturability can be detected by pretreatment or coadministration with nonradioactive homologous compound,<sup>19</sup> in this case bexarotene. The lack of observable saturation of [ $^{11}\text{C}$ ]bexarotene uptake by PET imaging does not indicate an absence of specific interactions with targets such as RXR, but rather a high proportion of nonsaturable uptake, possibly including interactions with lipid membranes in the CNS.<sup>20</sup> Evidence also suggests that bexarotene may engage in specific interactions with multiple high-expression targets in addition to RXR hetero- and homodimers,<sup>21-23</sup> which could contribute to the observed sustained uptake under drug coadministration conditions.

The high lipophilicity of RXR ligands presents a challenge for the development of molecular imaging agents that demonstrate highly specific uptake in vivo. The measured  $\log D$  of [ $^{11}\text{C}$ ]bexarotene (3.68) falls somewhat outside the typical range for successful PET neuroimaging agents that cross the blood-brain barrier (0.9-2.5).<sup>24,25</sup> Despite a higher than ideal  $\log D$  value and nearly total plasma protein binding, [ $^{11}\text{C}$ ]bexarotene shows reasonable brain uptake in both rat and NHP. Due to the highly lipophilic binding site, and apparent promiscuity of known RXR ligands, development of a suitable radiotracer for neuroimaging may not be a practical goal at this time. Future efforts to develop molecular imaging probes for RXR will need to prioritize less lipophilic compounds to improve on brain extraction fraction and binding specificity in addition to the target selectivity. As interests in RXR-mediated mechanisms for

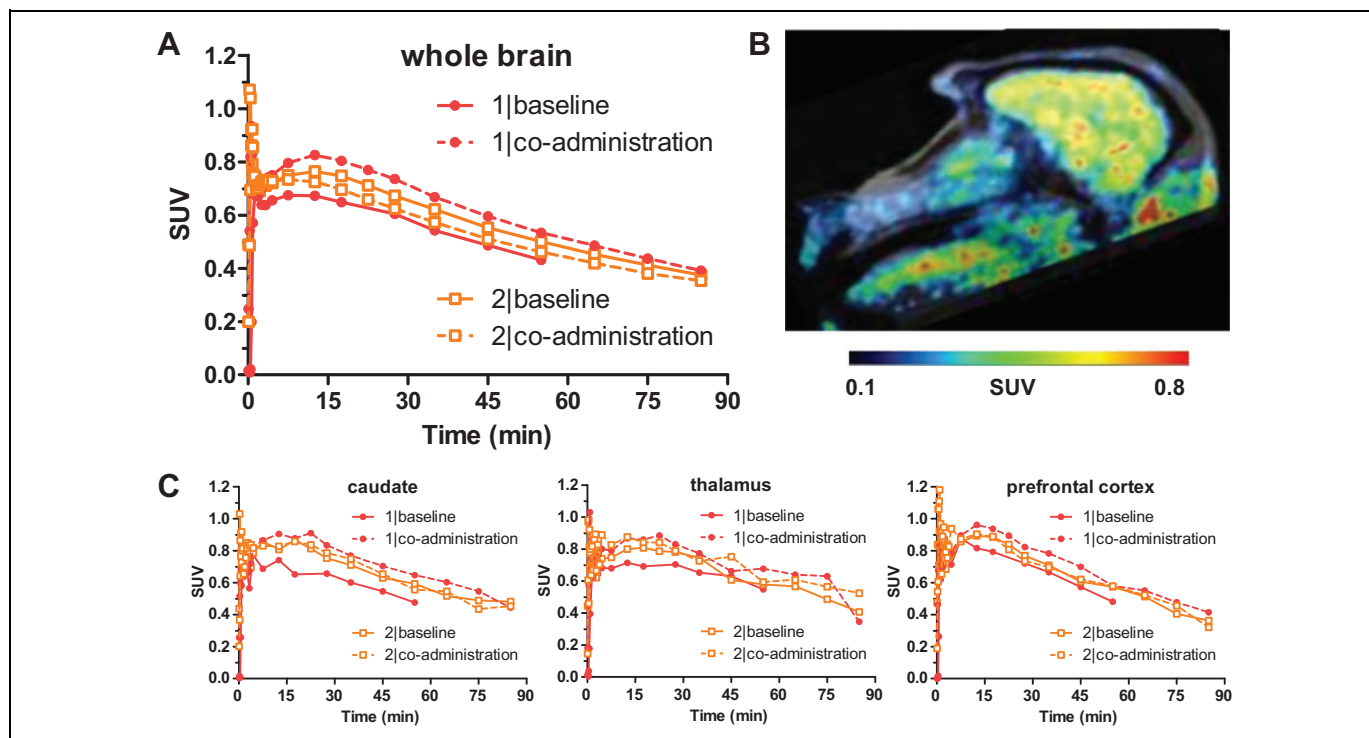


**Figure 2.** A, Whole-brain PET time-activity curves of [ $^{11}\text{C}$ ]bexarotene in nonhuman primate at baseline and with coadministration of bexarotene (0.35–0.42 mg/kg, IV,  $n = 2$ ). B, Summed PET-MR sagittal image at baseline 30 to 60 minutes. C, Regional time-activity curves for select brain VOIs. IV indicates intravenously; MR, magnetic resonance; PET, positron emission tomography; VOIs, volumes of interest.

the treatment of AD and PD are actively pursued, it is anticipated that new compounds under development will possess superior properties for CNS targeting of RXRs and provide an improved platform for radiotracer development for this important target.

### Acknowledgments

The authors are grateful to Helen Deng, Brendan Taillon, and Martinos Center radiopharmacy and imaging staff (Grae Arabasz, Garima Gautham, Shirley Hsu, Kari Phan, Judit Sore, and Samantha To) for help with radiochemistry and imaging experiments. Acknowledgment is given to Dr Martin Sanders and Dr Rosh Chandraratna for helpful discussions.

### Declaration of Conflicting Interests

The author(s) declared no potential conflicts of interest with respect to the research, authorship, and/or publication of this article.

### Funding

The author(s) disclosed receipt of the following financial support for the research, authorship, and/or publication of this article: Research was supported by the Michael J. Fox Foundation (grant #11786). S.H.L. is a recipient of NIH career development award (DA038000).

### References

- McFarland K, Spalding TA, Hubbard D, Ma JN, Olsson R, Burstein ES. Low dose bexarotene treatment rescues dopamine neurons and restores behavioral function in models of Parkinson's disease. *ACS Chem Neurosci*. 2013;4(11):1430-1438.
- Cramer PE, Cirrito JR, Wesson DW, et al. ApoE-directed therapeutics rapidly clear  $\beta$ -amyloid and reverse deficits in AD mouse models. *Science*. 2012;335(6075):1503-1506.
- Boehm MF, Zhang L, Badea BA, et al. Synthesis and structure-activity relationships of novel retinoid X receptor-selective retinoids. *J Med Chem*. 1994;37(18):2930-2941.
- Cummings JL, Zhong K, Kinney JW, et al. Double-blind, placebo-controlled, proof-of-concept trial of bexarotene in moderate Alzheimer's disease. *Alzheimers Res Ther*. 2016;8:4.
- Farol LT, Hymes KB. Bexarotene: a clinical review. *Expert Rev Anticancer Ther*. 2004;4(2):180-188.
- Assaf C, Bagot M, Dummer R, et al. Minimizing adverse side-effects of oral bexarotene in cutaneous T-cell lymphoma: an expert opinion. *Br J Dermatol*. 2006;155(2):261-266.
- Lerner V, Miodownik C, Gibel A, et al. Bexarotene as add-on to antipsychotic treatment in schizophrenia patients: a pilot open-label trial. *Clin Neuropharmacol*. 2008;31(1):25-33.
- Lerner V, Miodownik C, Gibel A, et al. The retinoid X receptor agonist bexarotene relieves positive symptoms of schizophrenia: a 6-week, randomized, double-blind, placebo-controlled multicenter trial. *J Clin Psychiatry*. 2013;74(12):1224-1232.
- Rotstein BH, Hooker JM, Woo J, et al. Synthesis of [ $^{11}\text{C}$ ]bexarotene by Cu-mediated [ $^{11}\text{C}$ ]carbon dioxide fixation and preliminary PET imaging. *ACS Med Chem Lett*. 2014;5(6):668-672.
- Takashima-Hirano M, Ishii H, Suzuki M. Synthesis of [ $^{11}\text{C}$ ]Am80 via novel Pd(0)-mediated rapid [ $^{11}\text{C}$ ]carbonylation using arylboronate and [ $^{11}\text{C}$ ]carbon monoxide. *ACS Med Chem Lett*. 2012;3(10):804-807.

11. Suzuki M, Takashima-Hirano M, Ishii H, et al. Synthesis of  $^{11}\text{C}$ -labeled retinoic acid, [ $^{11}\text{C}$ ]ATRA, via an alkenylboron precursor by Pd(0)-mediated rapid C-[ $^{11}\text{C}$ ]methylation. *Bioorg Med Chem Lett*. 2014;24(15):3622-3625.
12. Wang M, Davis T, Gao M, Zheng QH. Synthesis of a new fluorine-18-labeled bexarotene analogue for PET imaging of retinoid X receptor. *Bioorg Med Chem Lett*. 2014;24(7):1742-1747.
13. Mangelsdorf DJ, Borgmeyer U, Heyman RA, et al. Characterization of three RXR genes that mediate the action of 9-cis retinoic acid. *Genes Dev*. 1992;6(3):329-344.
14. Moreno S, Farioli-Vecchioli S, Cerù MP. Immunolocalization of peroxisome proliferator-activated receptors and retinoid x receptors in the adult rat CNS. *Neuroscience*. 2004;123(1):131-145.
15. Toporova L, Macejova D, Brtko J. Radioligand binding assay for accurate determination of nuclear retinoid X receptors: a case of triorganotin endocrine disrupting ligands. *Toxicol Lett*. 2016;254:32-36.
16. Riss PJ, Lu S, Telu S, et al. Cu<sup>I</sup>-catalyzed  $^{11}\text{C}$  carboxylation of boronic acid esters: a rapid and convenient entry to  $^{11}\text{C}$ -labeled carboxylic acids, esters, and amides. *Angew Chem Int Ed Engl*. 2012;51(11):2698-2702.
17. Rotstein BH, Liang SH, Holland JP, et al.  $^{11}\text{CO}_2$  fixation: a renaissance in PET radiochemistry. *Chem Commun*. 2013;49(50):5621-5629.
18. Wong SF. Oral bexarotene in the treatment of cutaneous T-cell lymphoma. *Ann Pharmacother*. 2001;35(9):1056-1065.
19. Van de Bittner GC, Ricq EL, Hooker JM. A philosophy for CNS radiotracer design. *Acc Chem Res*. 2014;47(10):3127-3134.
20. Fantini J, Di Scala C, Yahi N, et al. Bexarotene blocks calcium-permeable ion channels formed by neurotoxic Alzheimer's  $\beta$ -amyloid peptides. *ACS Chem Neurosci*. 2014;5(3):216-224.
21. Boergesen M, Pedersen TÅ, Gross B, et al. Genome-wide profiling of liver x receptor, retinoid x receptor, and peroxisome proliferator-activated receptor  $\alpha$  in mouse liver reveals extensive sharing of binding sites. *Mol Cell Biol*. 2012;32(4):852-867.
22. Kim M-S, Lim DY, Kim J-E, et al. Src is a novel potential off-target of RXR agonists, 9-cis-UAB30 and Targretin, in human breast cancer cells. *Mol Carcinog*. 2015;54(12):1596-1604.
23. Marciano DP, Kuruvilla DS, Pascal BD, et al. Identification of bexarotene as a PPAR antagonist with HDX [Published online September 15, 2015]. *PPAR Res*. 2015;e254560.
24. Dischino DD, Welch MJ, Kilbourn MR, et al. Relationship between lipophilicity and brain extraction of C-11-labeled radiopharmaceuticals. *J Nucl Med*. 1983;24:1030-1038.
25. Waterhouse RN. Determination of lipophilicity and its use as a predictor of blood-brain barrier penetration of molecular imaging agents. *Mol Imaging Biol*. 2003;5(6):376-389.